On the interaction of a rigid / flexible manipulator with a compliant surface

Atef A. Ata and Saad S. A. Ghazy
Mathematical Eng. Dept., Faculty of Eng., Alexandria University, Alexandria (21544), Egypt

Constrained maneuver of a two link hybrid manipulator with one flexible link is considered in this study. The second flexible link is in contact with a compliant surface. The surface can move freely parallel to itself by changing the hinged point along the X-axis and can also rotate about the pivot. The effect of the force exerted at the end effector of the flexible arm and on the required hub torque is investigated for different values of the inclination angle and the position of the compliant surface. The mathematical model of for the hybrid robot arm is obtained by the extended Hamilton's principle. The required hub torque for the constrained maneuvers are obtained through the solution of the inverse dynamics problem without ignoring the nonlinear terms of the equations of motion. The contact force and the required hub torque to move the end effector through a prescribed trajectory are calculated for many cases to better select the optimum performance parameters.

الغرض من هذا البحث هو دراسة الحركة المقيدة لإنسان الي مكون من عضوين الأول جاسيء والثاني مرن. يتصل بـــللعضو المرن عند نهايته كتلة طرفية تتحرك بحيث تكون ملامسة دائما لسطح مطيع. هذا السطح يمكنه الانتقال موازيا لنفســـه علـــي المحور الأفقي وذلك بتغيير نقطة تثبيته مع الأرض. فضلا عن ذلك ، يكنه الدوران أيضا حول نقطة التثبيت. في هذا البحـــث يتم دراسة مدى تاثير زاوية ميل المستوى وكذلك بعد نقطة تثبيته مع المستوى الأفقي علي القوة المتولدة نتيجة التلامس بيـــن الكتلة الطرفية والمستوي المائل وكذلك علي عزم الدوران اللازم لتحريك الكتلة الطرفية خلال مسار معـــد ســـلفا. النمـــوذج الرياضي للمجموعة تم استنتاجه باستخدام مبدأ هاملتون الممتد. تم الحصول على قوى التلامس وكذلك العزم اللازم لكل عضو عن طريق حل مسألة الديناميكا المقابلة. كذلك تم تطبيق الطريقة علي ثلاث حالات مختلفة للوصول إلى أنسب متغيرات تحكم أداء الإنسان الالي في العمليات المختلفة.

Keywords: Hybrid robot, Compliant surface, Inverse dynamics, Contact force, Analytical solution

1. Introduction

A robot is considered to be in constrained motion when its end effector contacts and / or interacts with the environment as the robot arm moves. The control objectives, in this case, are trajectory tracking and force regulation. Typical examples of such constrained robots include grinding, cutting, drilling, inserting, fastening, contour following, etc. So, it is important to investigate how the inclination angle of the compliant surface can affect the force exerted at the end effector and the required joints torque for different tasks.

Force/motion control of constrained robot was first addressed by assuming exact knowledge of the robot dynamic model. Raibert and Craig [1] applied hybrid position/force control for rigid manipulator. In 1985, Maples [2] investigated the problem of contact force control at one end of a very flexible arm by controlling the torque at the other end. Tilley and Cannon [3] discovered that a great improvement could be obtained in the behavior of a one-degree of freedom wrist using a fast micromanipulator at the end of a very flexible robot. Tilley et al. [4] continued their work towards two degree- of-freedom wrist. It was expected to have better performance although it was not experimentally proved.

More recently, the research is extended to force / motion control of constrained robots with parameter uncertainties. Chiou and Shahinpoor [5] studied the stability of

constrained flexible manipulators. Su et al. [6] proposed a control algorithm for constrained motion of a two link hybrid robot using feedforward and feedback torque and simulation results were also presented. Spong [7] and Jankowsky and ElMaraghy [8] studied force control of flexible joint manipulators. However, the performance of the force controlled flexible manipulators is limited since the response of the tip of the flexible manipulators is generally slow, and simultaneous position force control at the tip is difficult. While, Yao et al. [9] addressed the motion and force tracking control of robot manipulator in contact with a compliant surface with unknown stiffness. In 1998, Yao and Tomizuka [10] continued their work by considering the high performance robust motion and force tracking control of a two link rigid robot in contact with a compliant surface. Yoshikawa et al. [11] proposed hybrid position/force control algorithm of combined flexible-macro/rigid-micro manipulator system. The macro part is controlled to compensate for the position and force errors due to elasticity in the macro part. Ata [12] addressed the problem of constrained maneuvers of a hybrid manipulator with variable tip mass in contact with a fixed vertical constraint It was discovered that while the influence of the variation of tip mass appears only at high accelerations, the contact force has a great effect on the required torque for both links.

In practice, parameters of the system such as gravitational load and the stiffness of the contact surface vary from task to another. So, it is the object of this study to investigate the effect of the inclination angle of the contact surface and its position on the force exerted between the end effector and the compliant surface and on the required hub torque through the solution of the inverse dynamics problem. Simulation is carried out for different values of inclination angles and the compliant surface positions along the X-axis to define the range for optimum performance in the open loop case.

2. Problem formulation

Consider a two-link hybrid robot as shown in fig. 1. The robot consists of a rigid link attached to a rigid hub while the second link is assumed to be flexible. The mass densities of the rigid and flexible links are ρ_1 and ρ_2 respectively. At the distal end there is a tip mass (M_{tp}), including the wrist and the object mass, with moment of inertia (I_{tp}) about its own axis of rotation. The end effector is in contact with an inclined compliant surface. It is assumed that the compliant surface intersects the X-axis at three arbitrary positions respectively (R_x). In addition to, the compliant surface can also rotate about the hinged point (point of intersection with the X-axis) for four different angles (α).

The flexible link is modeled using Euler-Bernoulli's beam theory where shear deformation and rotary inertia can be neglected. The Virtual Link Coordinate System is applied and the angle $\theta_2(t)$ is considered as the angle between the virtual link and the horizontal. Because of the selection of the rigid body coordinates, the end point position of the beam can be expressed by the rigid body mode variable alone. This simple representation of the end point position enables the simple derivation of the inverse dynamics equation.

Applying the Virtual Link Coordinate System, The Lagrangian of the system can be divided into rigid and flexible parts as follow [13]:

$$L = L_r + L_f, \tag{1}$$

in which L_r is the Lagrangian due to the rigid motion, L_f is due to the flexibility effect and $\bar{L}_f$ is the Lagrangian density and can be given by:

$$L_f = \int_0^{\ell_2} \bar{L}_f dx. \tag{2}$$

For the hybrid manipulator system with tip mass under consideration these terms take the form [for more details, see [13] and [21],

$$L_{1r} = 0.5(I_{b1} + I_{h1})\dot{\theta}_1^{\,2} - m_1\bar{x}_1 g \sin\theta_1 , \qquad (3\text{-a})$$

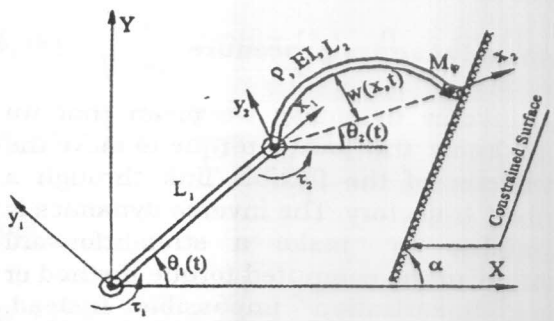

Fig. 1. Two links Hybrid manipulator

$$L_{2r} = 0.5m_2\ell_1^{\,2}\dot{\theta}_1^{\,2} + 0.5(I_{b2} + I_{h2})\dot{\theta}_2^{\,2} + m_2\ell_1\bar{x}_2\dot{\theta}_1\dot{\theta}_2\cos(\theta_2 - \theta_1) - m_2\bar{x}_2 g\sin\theta_2 - m_2 g\ell_1\sin\theta_1, \qquad (3\text{-b})$$

$$\bar{L}_f = 0.5\rho_2\left[W^2\dot{\theta}_2^{\,2} + \dot{W}^2 + 2x\dot{W}\dot{\theta}_2 + 2\ell_1\dot{\theta}_1[\dot{W}\cos(\theta_2 - \theta_1) - W\dot{\theta}_2\sin(\theta_2 - \theta_1)]\right] - 0.5EI\left(\frac{\partial^2 W}{\partial x^2}\right)^2 - \rho_2 g W\cos\theta. \qquad (3\text{-c})$$

Where:

$$I_{b1} = \int_0^{\ell_1}\rho_1 x^2 dx , \qquad (4\text{-a})$$

$$I_{b2} = \int_0^{\ell_2}\rho_2 x^2 dx , \qquad (4\text{-b})$$

$$m\bar{x}_2 = \int_0^{\ell_2}\rho_2 x dx . \qquad (4\text{-c})$$

I_{b1}, I_{h1}, I_{b2} and I_{h2} are the beam and hub Inertia's of the first and second Link, respectively.

M_{tp} is the a tip mass including the wrist and the object mass,

I_{tp} is the moment of inertia of the tip mass about its own axis of rotation

In our case, then, the Lagrangian of the system will be:

$$L = L_{1r} + L_{2r} + L_{M_{tp}r} + L_f . \qquad (5)$$

The equations of motion in Lagrangian form can be written in the form [13]:

$$\frac{\partial L}{\partial\theta} - \frac{d}{dt}\left(\frac{\partial L}{\partial\dot{\theta}}\right) + Q = 0 , \qquad (6)$$

$$\frac{\partial L_f}{\partial W} - \frac{d}{dt}\left(\frac{\partial L_f}{\partial\dot{W}}\right) + \frac{\partial^2}{\partial x^2}\left(\frac{\partial L_f}{\partial W''}\right) = 0 . \qquad (7)$$

Subject to the boundary conditions

$$\{W(0,t)\} = 0 , \qquad (8\text{-a})$$

$$\{W(\ell_2,t)\} = 0 , \qquad (8\text{-b})$$

$$\frac{\partial\bar{L}_f(0)}{\partial W''} - \tau_{2,1} = 0 , \qquad (8\text{-c})$$

$$\frac{\partial\bar{L}_f(\ell_2)}{\partial W''} - \tau_{2,3} = 0 . \qquad (8\text{-d})$$

Where

$\tau_{2,1}$ & $\tau_{2,3}$ are the flexible hub torques at the proximal and distal ends of the flexible arm.

Q is the generalized torque.

Upon substituting from eqs. (2-5) into eqs. (6-8) and after some algebraic manipulation, one can get the equations of motion and the corresponding boundary conditions as:

$$I_{tot1}\ddot{\theta}_1 + m_2\ell_1\bar{x}_2[\ddot{\theta}_2\cos(\theta_2 - \theta_1) - \dot{\theta}_2^{\,2}\sin(\theta_2 - \theta_1)] + (m_1\bar{x}_1 + m_2\ell_1 - M_{tp}\ell_1)g\cos_1 + \ell_1\int_0^{\ell_2}\rho_2[\ddot{W} - W\dot{\theta}_2^{\,2}]\cos(\theta_2 - \theta_1)_{dx} - [W\ddot{\theta}_2 + 2\dot{W}\dot{\theta}]\sin(\theta_2 - \theta_1) + M_{tp}\ell_1\ell_2[\ddot{\theta}_2\cos(\theta_2 - \theta_1) - \dot{\theta}_2^{\,2}\sin(\theta_2 - \theta_1)] - Q_1 = 0, \qquad (9)$$

$$I_{tot2}\ddot{\theta}_2 + m_2\ell_1\bar{x}_2[\ddot{\theta}_1\cos(\theta_2-\theta_1) - \dot{\theta}_1^2\sin(\theta_2-\theta_1)] + (m_2\bar{x}_2 + M_{tp}\ell_2)g\cos_2 + \ell_1\int_0^{\ell_2}\rho_2([W^2\ddot{\theta}_2 + 2W\dot{W}\dot{\theta}_2 + x\ddot{W}] + \ell_1 W[\dot{\theta}_1^2\cos(\theta_2-\theta_1) - \ddot{\theta}_1\sin(\theta_2-\theta_1)] - gW\sin\theta_2)dx + M_{tp}\ell_1\ell_2[\ddot{\theta}_1\cos(\theta_2-\theta_1) - \dot{\theta}_1^2\sin(\theta_2-\theta_1)] - Q_2 = 0, \quad (10)$$

$$\rho_2\left[W\dot{\theta}_2^2 - \ddot{W} - x\ddot{\theta}_2 - g\cos\theta_2 - \ell_1[\ddot{\theta}_1\cos(\theta_2-\theta_1) + \dot{\theta}_1^2\sin(\theta_2-\theta_1)\right] - EI\frac{\partial^4 W}{\partial x^4} = 0. \quad (11)$$

Where;

$$I_{tot1} = I_{b1} + I_{h1} + I_{tp} + M_{tp}\ell_1^2,$$

$$I_{tot2} = I_{b2} + I_{h2} + I_{tp} + M_{tp}\ell_2^2,$$

$$Q_1 = \tau_1 - F_x[\ell_1\sin\theta_1 + \ell_2\sin\theta_2] + F_y[\ell_1\cos\theta_1 + \ell_2\cos\theta_2], \text{and} \quad (12)$$

$$Q_2 = \tau_2 - F_x[\ell_2\sin\theta_2] + F_y[\ell_2\cos\theta_2]. \quad (13)$$

In order to obtain an accurate model with a small number of modes, it is advised to consider more accurate boundary conditions due to the absence of a rigid hub at the distal end and the existence of the tip mass with inertia instead. So, the boundary conditions will take into considerations these changes [14,15].

$$\{W(0,t)\} = 0, \quad (14\text{-a})$$

$$\{W(\ell_2,t)\} = 0, \quad (14\text{-b})$$

$$-EI\frac{\partial^2 W}{\partial x^2}(0) - \tau_2 = 0, \quad (14\text{-c})$$

$$EI\frac{\partial^2 W}{\partial x^2}(\ell_2) = \frac{I_{tp}}{I_{b1}}\beta^4\phi'(\ell_2). \quad (14\text{-d})$$

Where:

β is the eigenvalue and $\phi(x)$ is the corresponding mode shape and will be given in details in the next section.

3. Inverse dynamics procedure

By inverse dynamics we mean that we want to know the joints torque to move the end effector of the flexible link through a prescribed trajectory. The inverse dynamics is so complex to make a straightforward application of the computed torque method or feedback linearization impossible. Instead, some approximate schemes are proposed for open and closed loop control [16]. In our case, solving eqs. (9-11) for the joints torque subject to the boundary conditions(14-a-14-d) to obtain the flexible hub torque is a very difficult task if it is not impossible. This is simply because one has to calculate the elastic deflection of the arm to obtain the flexible hub torque. Unfortunately the required hub torque for the flexible link is also included in the boundary condition (14-c). An alternative approach to the computation of the link deformation is to use approximations for the flexible torque as suggested by Asada [16]. One can assume the second arm is rigid, substituting the joint angle, obtaining the hub torque for the virtually rigid arm. The resultant torque can be used as an approximate for the flexible arm model. The final step is to substitute into eq. (10) to obtain the desired flexible hub torque. To simplify the manipulation of the solution, consider the substitution:

$$Y(x,t) = W(x,t) + x\theta(t). \quad (15)$$

Which represents the total deflection of the flexible arm. By substituting equation (15) into eqs. (9,10,12, 14), one can solve for the total deflection instead of the flexible deflection (for more details see [17]). The differential equation is then transformed to a non-homogeneous differential equation with homogeneous boundary conditions. Applying

the assumed mode method [18], $Y(x,t)$ can be given in the form:

$$Y_n(x,t) = \sum_{n=1}^{\infty} \phi_n(x) C_n(t) + A_n(x)\theta_2(t) + \frac{B_n(x)}{EI}\tau_2 . \quad (16)$$

Where;

$$\phi_n(x) = \sqrt{\frac{2}{\rho AL}} \sin(\beta x / L), \quad \beta_n = n\pi / L,$$

$$A_n(x) = (2x - \frac{2x^3}{L^2} + \frac{x^4}{L^3}) / L,$$

and

$$B_n(x) = (-\frac{Lx}{3} + \frac{x^2}{2} - \frac{x^3}{6L}) .$$

Where $A_n(x)$ and $B_n(x)$ are functions of the state variable x alone that render the non-homogeneous boundary conditions into homogeneous boundary conditions. $\phi_n(x)$ is the mode shape and $C_n(t)$ is the time dependent boundary function.

Neglecting the first nonlinear term of eq. (11), since its effect is obvious only at very high speeds, The last two nonlinear terms inside the parentheses can be regarded as distributed excitation force with unit density [18]. This effect can be compensated in the time function as:

$$C_n(t) = \frac{1}{\omega_d} \int_0^t N_n(t) \sin \omega_d (t-\tau) \, EXP[-\zeta\omega_n(t-\tau)] d\tau, \quad (17)$$

where:

$$N_n(t) = N_{n1}(t) - \ell_1 \int_0^{\ell_2} \varphi_n(x)[\ddot{\theta}_1 \cos(\theta_2 - \theta_1) + \dot{\theta}_1^2 \sin(\theta_2 - \theta_1)]dx$$

$$N_{n1}(t) = -\left[G_{ni}^*(x)\ell_2\theta_2(t) + G_{ni}(x)\ell_2\ddot{\theta}_2(t)\right] - \left[H_{nj}^*(x)\frac{\tau_2(t)}{EI} + H_{nj}\frac{\ddot{\tau}_2(t)}{EI}\right],$$

in which;

$$G_{ni} = \int_0^{\ell_2} \rho\phi_n(x) A_n(x) dx ,$$

$$G^*_{ni} = \int_0^{\ell_2} \phi_n(x) \frac{\partial^4 (A_n(x))}{\partial x^4} dx ,$$

$$H_{nj} = \int_0^{\ell_2} \rho\phi_n(x) B_{nj}(x) dx ,$$

$$H^*_{nj} = \int_0^{\ell_2} \phi_n(x) \frac{\partial^4 (B_n(x))}{\partial x^4} dx .$$

In order to simulate the constrained motion, two different profiles of the joint angle are considered here. These profiles have common initial and final values. These trajectories represent a generic " pick- and – place" maneuver, whereby the manipulator starts from rest, accelerates gradually and then decelerates to stop. On the contrast they have different increasing rate and different acceleration profiles. These two trajectories are plotted in fig. 1 and the expressions for these profiles can be given as:

$$\theta_1 = 0.16(PI * t - \sin(PI * t)), \quad (18)$$

$$\theta_2 = 3(\frac{t}{2})^2 - 2(\frac{t}{2})^3 . \quad (19)$$

On the other hand, the contact force exerted by the robotic arm can be modeled by spring [1, 6]. If the horizontal position of the contact surface can be given in terms of the inclination angle α and the vertical displacement y in the form:

$$x = R_x + y / \tan\alpha ,$$

in which

$$y = \ell_1 \sin\theta_1 + \ell_2 \sin\theta_2 .$$

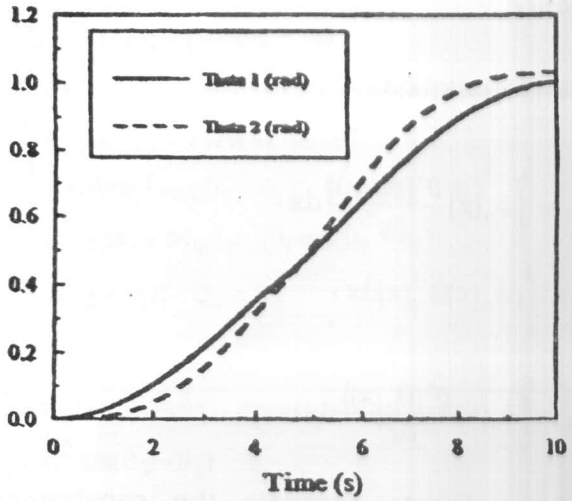

Fig. 2. Joints trajectories.

The contact force, including the inertia force due to tip mass, will be [5]

$$F = K_s[x - \ell_1 \cos\theta_1 - \ell_2 \cos\theta_2] + F_{iner}, \qquad (20)$$

where

$$F_{X\,iner} = M_{tp}[\ell_1 \sin\theta_1\ddot{\theta}_1 + \ell_2 \cos\theta_1\dot{\theta}_1^2 + \ell_2 \sin_2\ddot{\theta}_2 + \ell_2 \cos\theta_1\dot{\theta}_2^2],$$

$$F_{Y\,iner} = M_{tp}[\ell_1 \cos\theta_1\ddot{\theta}_1 - \ell_1 \sin\theta_1\dot{\theta}_1^2 + \ell_2 \cos_2\ddot{\theta}_2 - \ell_2 \sin\theta_1\dot{\theta}_2^2].$$

Where R_x is the position of the constraint surface and K_s is the spring stiffness which equals 1000 N/m. The selected system considered here is similar to that in [19] where the parameters of the system are:

$\ell_1 = \ell_2 = 0.65$,
$\rho_1 = \rho_2 = 0.3248 Kg/m$,
EI =1.831 N-m2 .

The hub inertia is assumed to be 10 times the beam inertia for both links [17, 20]. By substituting from eqs. (15-20) into eqs. (9 , 10) one can get the contact force and both rigid and flexible hub torques. In order to better select the optimum performance parameters of the constrained system, simulation is carried out for three cases employing the intersection points (R_x =1.3, 1.4, and 1.5 m) as a parameter. This can be done for four common rotating angles of the compliant surface (α =90,100,110 and 120 degrees) in each case. The results are illustrated in figs. 3, 4 and 5.

4. Discussion and conclusions

Enabling the compliant surface to rotate about the hinged point and to change the intersection point along the X-axis have a considerable effect on both the contact force and the seeking hub torques. This effect can be easily observed from figs. (3,4 and 5) for all the three cases.

1. In the first case, (R_x=1.3), Increasing the inclination angle α causes the end effector to lose contact with the compliant surface and returns to contact again within the time interval except for α =120.
2. for R_x=1.4 m, the initial distance results in an initial contact force between the end effector and the compliant surface. The contact force and both joints torque decrease as α increases. There is no worry about separation for the first three values of α since it occurs only at α =120 for a small period before it is disappear at the end of the time interval.
3. For the third case, where R_x=1.5 m no separation occurs at any value of α . On the other hand, the initial values of both hub torque may excite the unmodeled dynamics of the system. Also, as α increases some fluctuations in the contact force and both hub torque exist. This can be clearly observed for α =110 and 120.
4. For all the three cases above, the contact force and both hub torque reduce considerably as the angle of inclination increases.

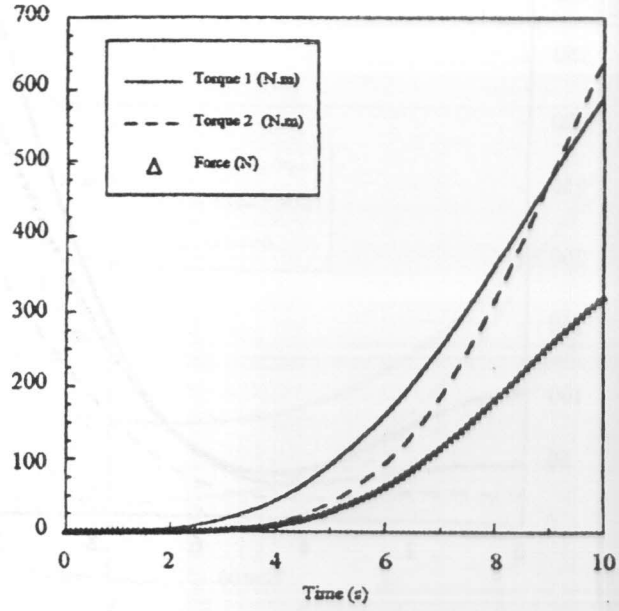

3-a. (RX=1.3, Angle =90)

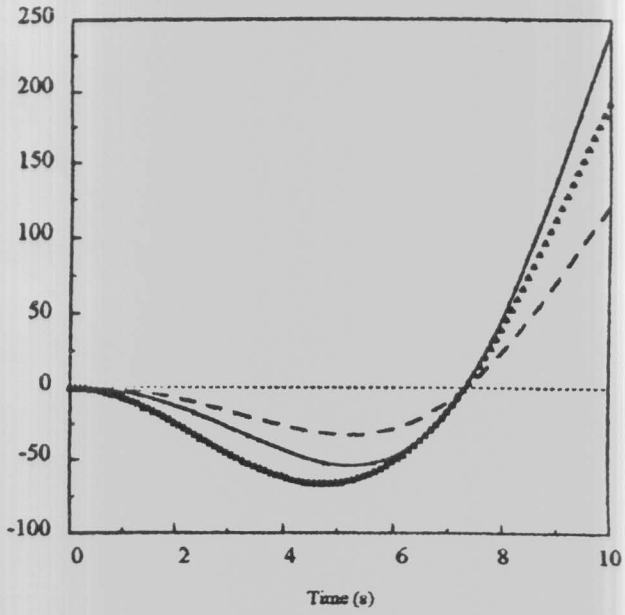

3-c. (RX=1.3, Angle=110)

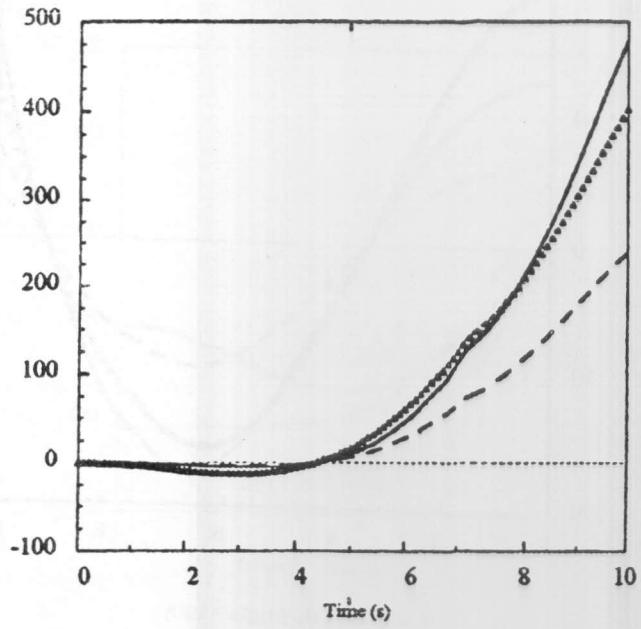

3-b. (RX=1.3, Angle=100)

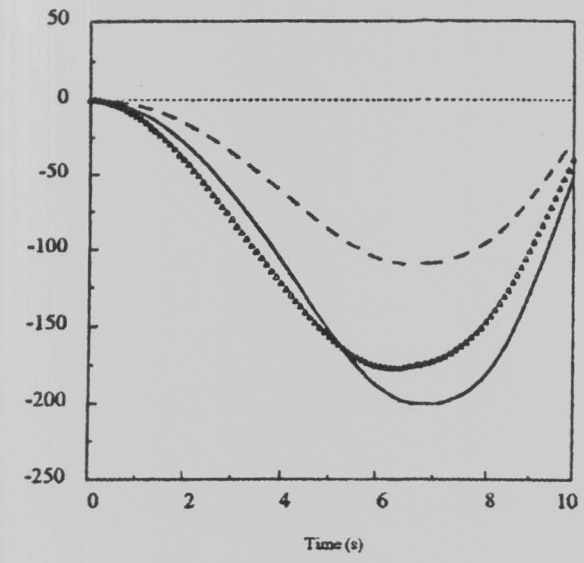

3-d. (RX=1.3, Angle=120)

Fig. 3. Contact force and joints torque.

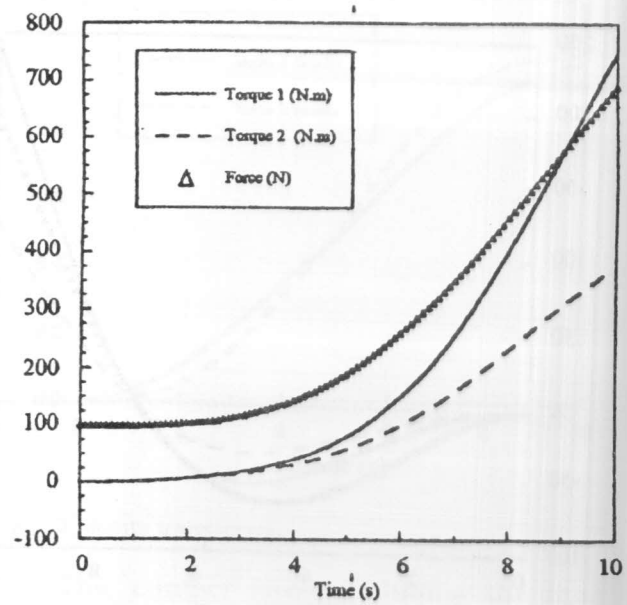

4-a. (RX=1.4, Angle =90).

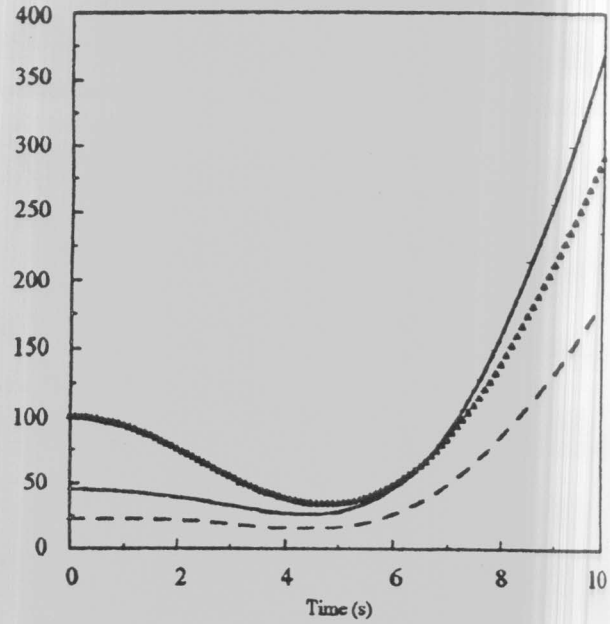

4-c (RX=1.4, Angle =110).

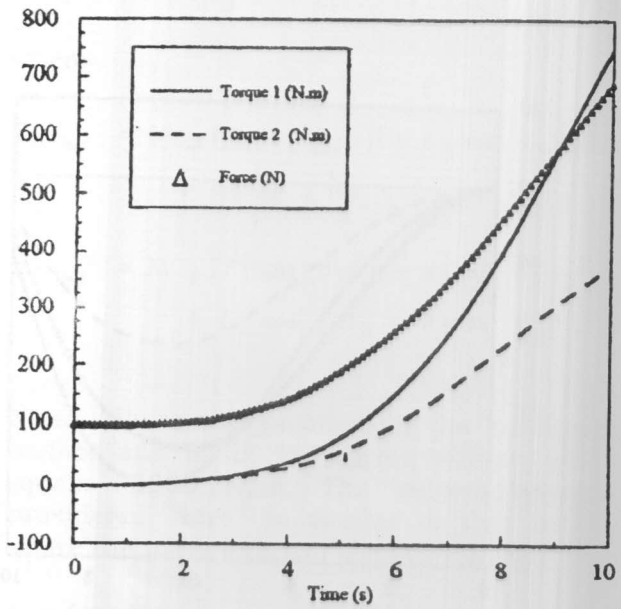

4-b. (RX=1.4, Angle =100)

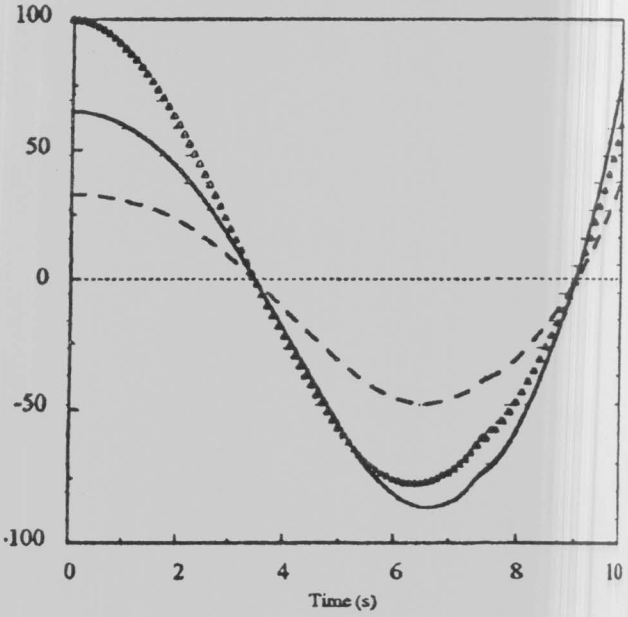

4-d (RX=1.4, Angle =120).

Fig. 4. Contact force and joints hub torque.

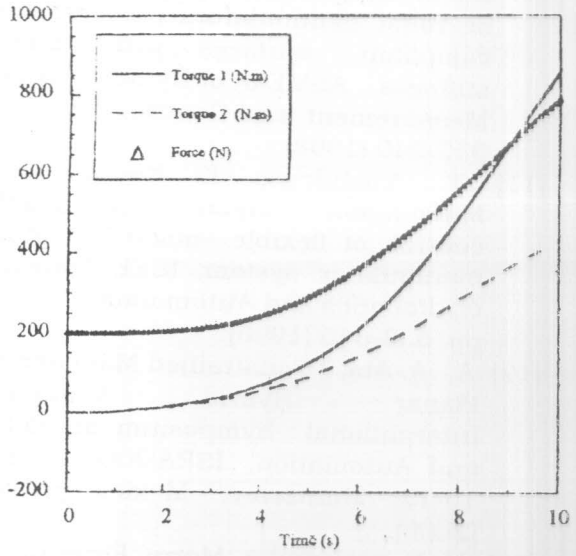

5-a. (RX=1.5, Angle=90).

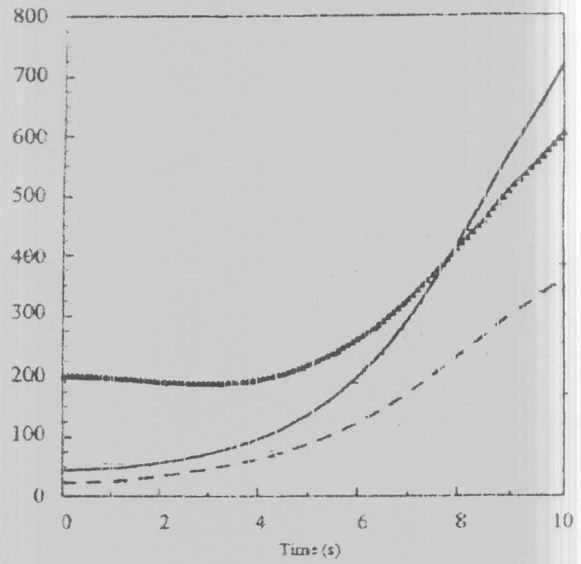

5-c. (RX=1.5, Angle=110).

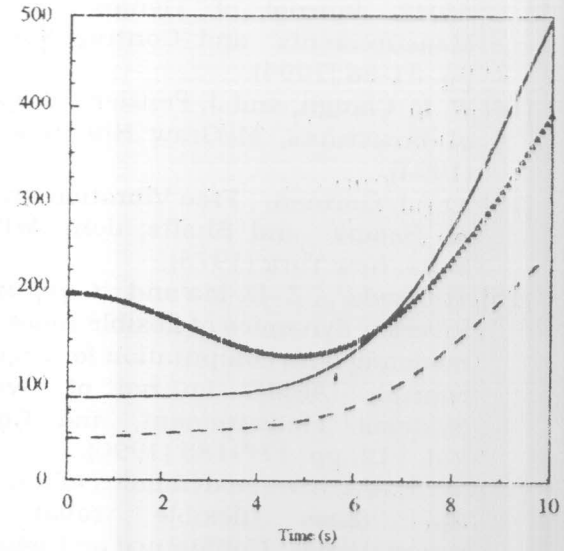

Fig. 5b. (RX=1.5, Angle=100).

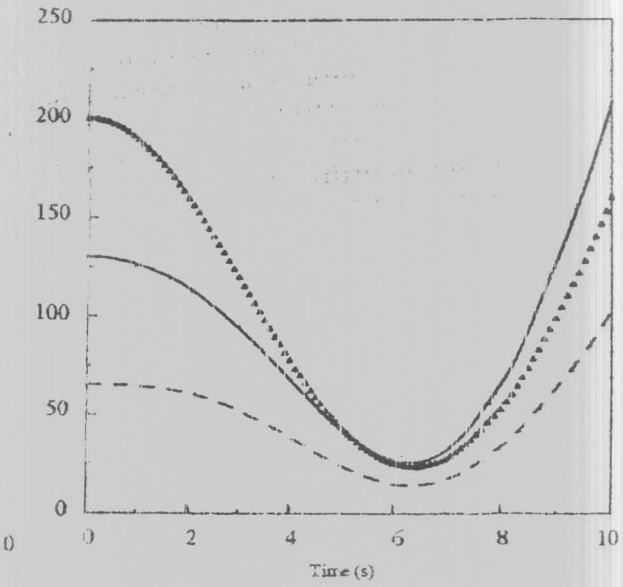

5-d. (RX=1.5, Angle=120

Fig.5. Contact force and joints toque.

References

[1] M. H. Raibert, and J. J. Craig , Hybrid position/force control of manipulators, ASME J. of Dynamic Systems, Measurement and Control, Vol. 102, pp. 126-133 (1981).

[2] J. A. Maples, Force control of robotic manipulators with structural flexibility Ph. D. Dissertation, Department of Electrical Engineering, Stanford University (1985).

[3] S. W. Tilley, and R. H. Cannon, Jr., Experiments on end-point position and force control of a flexible arm with a fast wrist, AIAA Guidance, navigation and Control Conf., pp. 41-49 (1986).

[4] S. W. Tilley, , R. H. Cannon, Jr. and R. Kraft, , End point force control of a very flexible manipulator with a fast end effector, Robotics: Theory and Applications, F. W. Paul and K. Yousef-Toumi, eds. DSC-Vol 3, ASME Winter Annual Meeting, pp. 1-9 (1986).

[5] B. C. Chiou, and M. Shahinpoor, Dynamic stability analysis of a two-link force-controlled flexible manipulator, Trans. ASME Journal of Dynamic Systems, Measurements and Control, Vol. 112, pp. 661-666 (1994).

[6] H. -J. Su, B. -O. Choi and K. Krishnamurthy : Force control of a high-speed, lightweight robotic manipulators, Math. Comput. Modeling, Vol. 14, pp. 474-479 (1990).

[7] M. Spong , On the force control problem of a constrained flexible robot arm," IEEE Transaction on Automatic Control, Vol. 34 (1), pp. 107-111 (1989).

[8] K. P. Jankowsky and H. A. ElMaraghy , "Dynamic decoupling for hybrid control of rigid-/flexible-joint robots interacting with the environment," IEEE Transaction on Robotics and Automation, Vol. RA-8 (5), pp. 519-534 (1992).

[9] B. Yao, S. P. Chan and D. Wang , Variable structure adaptive motion and force control of robot manipulators, Automatica, Vol. 30 (9), pp 1473-1477 (1994).

[10] B. Yao,., and M. Tomizuka , Adaptive robust motion and force tracking control of robot manipulators in contact with compliant surfaces with unknown stiffness, ASME J. of Dynamic Systems, Measurement and Control, Vol. 120, pp. 232-240 (1998).

[11] T. Yushikawa, K. Harada and A. Matsumoto, Hybrid position/force control of flexible -macro/ rigid-micro manipulator system, IEEE Transaction on Robotics and Automation, Vol. 12 (4), pp. 633-640 (1996).

[12] A. A. Ata, " Constrained Maneuvers of a Planar Hybrid Manipulator" International Symposium on Robotics and Automation, ISRA'2000, November 10-12, Monterrey, Mexico, pp. 63-68 (2000).

[13] M. Benati, and A. Morro, Formulation of the equations of motion for a chain of flexible links using Hamilton's principle, ASME Journal of Dynamic Systems, Measurements and Control, Vol. 116, pp. 81-88 (1994).

[14] W. R. Claugh, and J. Penzien , Dynamics of Structures, McGraw Hill, New York (1994).

[15] D. J. Gorman, , Free Vibration Analysis of Beams and Shafts, John Wiley & Sons, New York (1975).

[16] H. Asada , , Z.-D. Ma and H. Tokumaru, Inverse dynamics of flexible robot arms: modeling and computation for trajectory control, ASME Journal of Dynamic Systems Measurement, and Control, Vol. 112, pp. 177-185 (1990).

[17] A. A. Ata, Inverse dynamics of a variable tip mass flexible robot, 14th International Conference on Computer-Aided Production Engineering, CAPE'98, Tokyo, Sep. 8-10, pp. 493-498 (1998).

[18] L. Meirovitch, Analytical Methods in Vibration, Macmillan, New York (1967).

[19] E. Bayo, " Computed torque for the position control of open chain flexible robot" the IEEE Int. Conf. On Robotics and Automation, pp. 346-351 (1988).

[20] A. A. Ata, and S. M. ElKhoga , Effects of tip mass and actuator inertia on the behavior of a flexible arm robot, 1998 IEEE/IRS International conference on Intelligent Robots and Systems, Victoria, Canada, Vol. 1, pp 502-507 (1998).

[21] A. A. Ata, Inverse Dynamics and Control of a Single Link Flexible Manipulator, Ph. D. Thesis, Alexandria University, Egypt (1996)

Received: August 22, 2000
Accepted: February 26, 2001